Casado, Alberto; Radevici, Ivan; Sadi, Toufik; Oksanen, Jani

Temperature dependence of thermophotonic energy transfer in intracavity structures

Published in:
Photonic Heat Engines

DOI:
10.1117/12.2506227

Published: 01/01/2019

Document Version
Publisher's PDF, also known as Version of record

Please cite the original version:
Casado, A., Radevici, I., Sadi, T., & Oksanen, J. (2019). Temperature dependence of thermophotonic energy transfer in intracavity structures. In D. V. Seletskiy, R. I. Epstein, & M. Sheik-Bahae (Eds.), *Photonic Heat Engines: Science and Applications* (pp. 1-7). [109360U] (Proceedings of SPIE; Vol. 10936). https://doi.org/10.1117/12.2506227

PROCEEDINGS OF SPIE

SPIEDigitalLibrary.org/conference-proceedings-of-spie

Temperature dependence of thermophotonic energy transfer in intracavity structures

Alberto Casado, Ivan Radevici, Toufik Sadi, Jani Oksanen

Alberto Casado, Ivan Radevici, Toufik Sadi, Jani Oksanen, "Temperature dependence of thermophotonic energy transfer in intracavity structures," Proc. SPIE 10936, Photonic Heat Engines: Science and Applications, 109360U (1 March 2019); doi: 10.1117/12.2506227

SPIE.

Event: SPIE OPTO, 2019, San Francisco, California, United States

Temperature dependence of thermophotonic energy transfer in intracavity structures

Alberto Casado, Ivan Radevici, Toufik Sadi, and Jani Oksanen

Engineered Nanosystems Group, School of Science, Aalto University, P.O. Box 12200, FI-00076 AALTO, Finland

ABSTRACT

Electroluminescent cooling (ELC) of light–emitting diodes (LEDs) at high powers is yet to be demonstrated. Earlier studies of photoluminescent cooling (PLC) suggested that temperature strongly affects the light emission efficiency and therefore it is useful to explore the temperature range below room temperature (RT) where ELC might be easier to observe. With that purpose in mind, we electrically characterised three different sized (0.2, 0.5 and 1 mm diameter) double–diode structure (DDS) devices, consisting of a coupled LED and photodiode (PD), at temperatures ranging from 100 K to 325 K to investigate how the temperature affects the efficiency of the structures in practice. We found that, for the studied devices, the coupling quantum efficiency (CQE) as well as the overall efficiency indeed increase when temperature decreases and reach their highest values at temperatures below room temperature.

Keywords: Electroluminescent cooling, thermophotonic cooling, light-emitting diodes, temperature dependence, III-V semiconductors, heat engines

1. INTRODUCTION

Electroluminescent cooling (ELC) may enable a new class of efficient solid-state cooling technologies. Its working principle involves biasing a light–emitting diode (LED) at voltages below the active material band-gap energy so that the generation of photons requires the absorption of device thermal energy. Although ELC is relatively well understood,[1] and has been demonstrated at very low powers,[2] it is yet to be demonstrated at sufficiently high powers for practical applications.

One of the approaches to experimentally demonstrate high-power ELC consists of a double–diode structure (DDS),[3–5] a prototype device consisting of a coupled emitter – absorber structure as in Fig. 1. This configuration, using a DHJ LED as the emitter and a GaAs homojunction PD as the absorber, allows to confine light within the structure and avoid some of the common light-extraction difficulties. Additionally, the PD serves to directly probe the LED performance, as well as to estimate the lower limit for the photon-energy-transport efficiency.

When temperature decreases the efficiency of the LED should in principle increase.[6–8] However, it is more likely for a photon to absorb thermal energy from the lattice at higher temperatures. It is therefore hard to estimate the optimum temperature range only from general considerations, and there is a need to explore the optimal range experimentally. The aim of this work is to study the effect of temperature on the DDS behaviour and to identify the most suitable temperature range for the experimental observation of ELC at high powers. To this end, we explored the temperature dependence of the electrical behaviour of DDSs (with $Al_{0.3}Ga_{0.7}As$ barrier LEDs) within the range 100 K – 325 K, comparing three devices with different mesa areas.

2. EXPERIMENTAL DETAILS

2.1 DDS structure

The DDSs studied in this work consist of a double heterojunction (DHJ) GaAs/AlGaAs LED structures grown on top of a GaAs p-n-homojunction photodiode.[3] The basic device structure is shown in Fig. 1. Light emitted by the DHJ LED is guided towards the photodiode either directly or after reflection from the top contact. The epitaxial structures were fabricated by metalorganic vapour phase epitaxy (MOVPE). Each epistructure was processed to contain a selection of circular mesas of different diameters and contact regions. The contacts were formed by AuZn/Au and Ni/AuGe layers deposited on top of the p- and n-GaAs regions, respectively.

Photonic Heat Engines: Science and Applications, edited by Denis V. Seletskiy, Richard I. Epstein, Mansoor Sheik-Bahae, Proc. of SPIE Vol. 10936, 109360U
 · doi: 10.1117/12.2506227

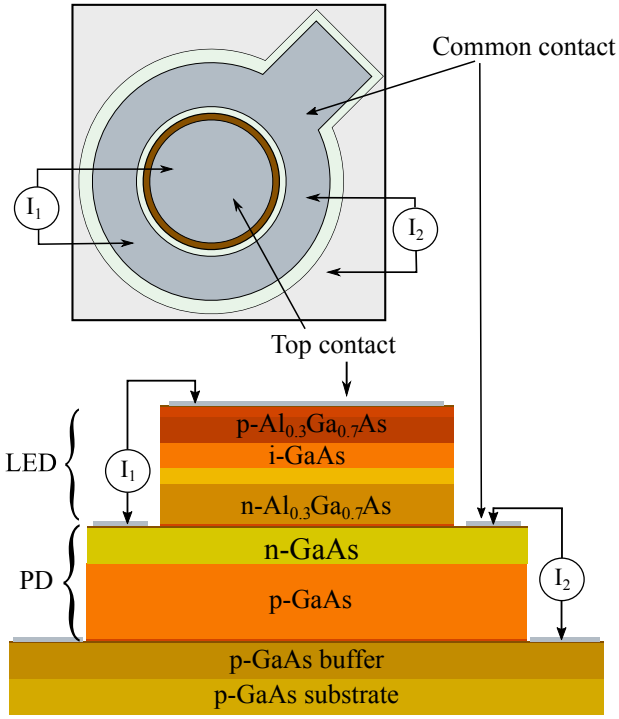

Figure 1: Top and side view of the DDS structure, and a representation of the $I-V$ curves measuring setup.

2.2 DDS characterisation

We characterised and analysed the behaviour of three DDS structures with diameters 0.2 mm, 0.5 mm and 1 mm, by simultaneously measuring the $I-V$ characteristics of the LED and the PD. The samples were placed inside a cryostat with a pressure $P \sim 5 \times 10^{-5}$ mbar and measured within the temperature range 100 K – 325 K in steps of 25 K. The temperature of the cold finger, onto which devices were attached, was measured by a calibrated sensor attached to the surface under the measured sample. The $I-V$ curves were obtained from a four-point probe setup (virtually avoiding the external resistance in the measurement wires), applying a voltage U_1 to the LED and simultaneously measuring I_1, the injected current through the LED, and I_2, the photogenerated current in the short-circuited photodiode ($U_2 \simeq 0$) when directly illuminated by the LED. Figure 1 shows the measurement setup schematics.

To extract basic information about the LED properties, we fitted our measurements to recombination models based on the ABC model, which is widely used to model the electrical characteristics of LEDs[9] and also provides the first order estimate of the temperature dependence of light emission. According to the model, there are three different channels of recombination in the LED active region: non-radiative Shockley-Read-Hall recombination (and similarly behaving interface/surface recombination), radiative recombination and Auger recombination, which are associated with three parameters A, B and C, respectively. The A coefficient was estimated, for all devices and temperatures, from the non-radiative (SRH-like) recombination dominated region in the $I-V$ curves using the expression

$$A = \frac{I_1}{qdan_i \cdot e^{\frac{qU_1}{2k_BT}}}, \tag{1}$$

where U_1 is the voltage over the LED, q is the elementary charge, k_B is the Boltzmann constant, d is the active-region thickness, a is the active-region area and n_i is the intrinsic charge concentration calculated as $n_i = \sqrt{N_C N_V}\exp[-qEg/(2k_BT)]$, N_C and N_V being the number of available states per unit volume in the conduction and valence band, respectively.

The evaluation of the LED internal quantum efficiency (IQE) in the DDS structure is based on the coupling quantum efficiency (CQE), a magnitude which represents an experimentally-measured lower limit of IQE. We define the CQE (or η_C) as

$$\eta_C = \frac{I_2}{I_1} \tag{2}$$

where I_2 is the photocurrent generated by the PD when I_1 is injected into the LED.

Additionally, the power–conversion efficiency (PCE) determines the lower limit for the electrical-energy-to-light conversion efficiency of the DDS and is defined as

$$\eta_{PC} = \frac{\hbar\omega}{qU_1} \cdot \eta_C \tag{3}$$

where $\hbar\omega$ is the average energy of the emitted photons. It can be stated that ELC is experimentally observed when $\eta_{PC} > 1$, i.e. $\hbar\omega\eta_C > qU_1$, corresponding to the case where the net heat absorption overcomes the internal heat generation in the LED.

3. RESULTS

3.1 $I - V$ curves

Figure 2a shows as an overview six representative $I-V$ curves (in a linear scale) of the three LEDs with diameters 0.2 mm (blue), 0.5 mm (green) and 1.0 mm (red) studied in this work, measured at 100 K and 300 K with the arrow representing the direction of increasing temperature. In addition to the temperature measured by the sensor, the devices actual temperature was estimated from the low voltage region of the $I - V$ curves with the expression $T = (q/nk_B) \times (\mathrm{d}U_1/\mathrm{d}[ln(I_1)])$, derived from the ideal diode equation. Assuming an ideality factor $n = 2$ in the previous expression, the difference between nominal and estimated values was lower than 10% for temperatures above 150 K and it gradually increased for lower temperatures. This could be a first indication of carrier freeze-out and/or a change of the ideality factor with temperature. As this needs further analysis of physical simulations and probably new measurements, we limit the results shown here to temperatures higher than 100 K.

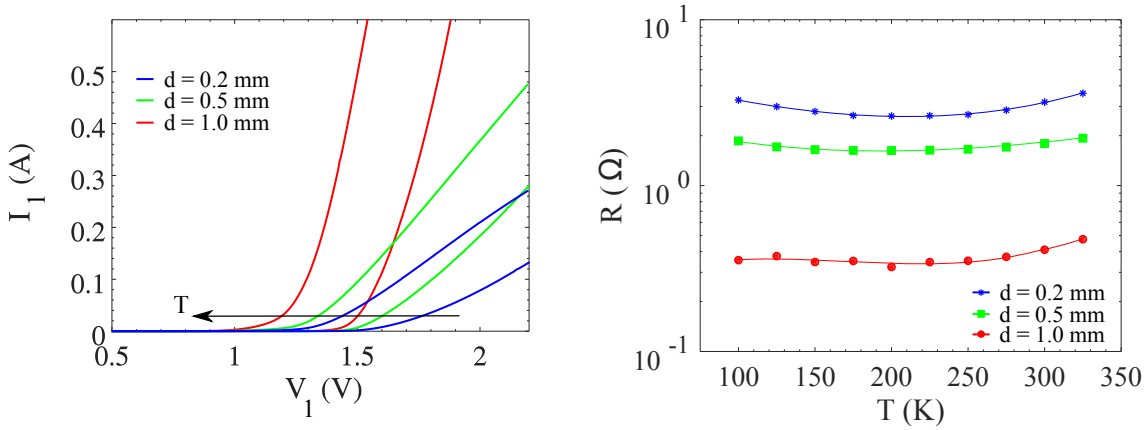

(a) (b)

Figure 2: (a) LED $I - V$ curves, measured at 100 K and 300 K, of the three studied devices with diameters d =(0.2, 0.5, 1.0) mm and (b) the dependence of their internal resistance with temperature.

The LED internal resistance, R, was calculated from the slope of the $I-V$ curves' resistance-dominated linear region at high biases, as $R = \Delta V/\Delta I$). Fig. 2b clearly shows a difference of around one order of magnitude

between the smallest and the largest device resistance due to the smaller active region volume with lower total recombination as well as the smaller circumference and larger resistance of the current spreading channel outside the mesa. Temperature variations, however, do not substantially influence the differential resistance.

Figure 3 shows the $I-V$ curves of (a) the 0.2-mm-diameter LED at all the temperatures measured (100 K – 300 K in steps of 25 K) and (b) for the three studied devices at 100 K, on logarithmic scale. The effect of surface recombination can be recognised in all the $I-V$ curves as a shoulder at voltages ranging between 1.3 and 1.5 V which, according to previous simulations and as presented in previous works,[4,5,10] might be due to the transition from a surface(mesa edge)-recombination to a bulk- and interface-recombination dominated region. The position and curvature of the shoulder varies with both temperature and device size.

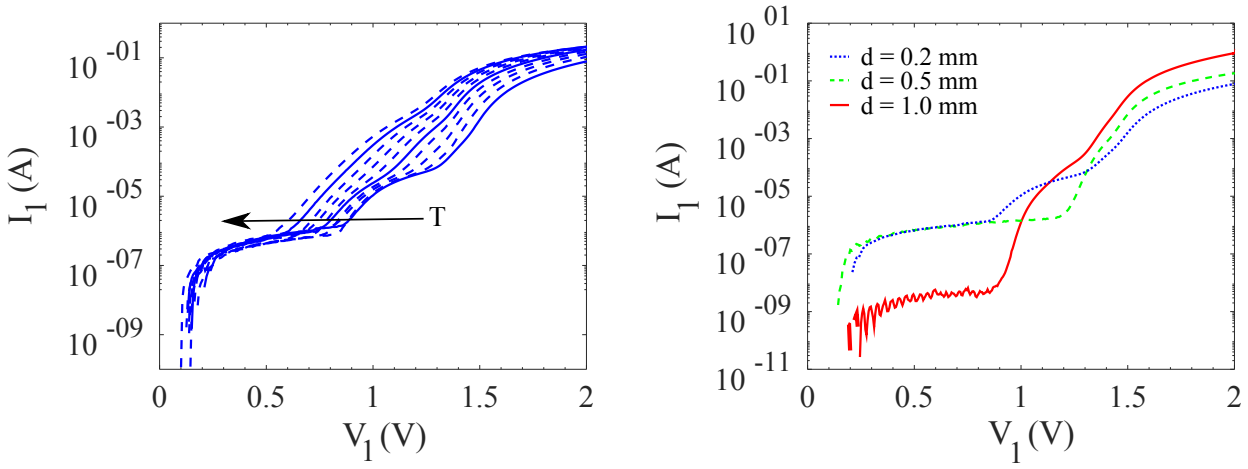

(a) (b)

Figure 3: Logarithmic scale $I-V$ curves of (a) the smallest device (0.2 mm diameter) at temperatures from 100 K to 325 K in steps of 25 K and (b) the three studied devices with diameters d =(0.2, 0.5, 1.0) mm at T = 100 K.

The shoulder associated with surface recombination becomes significantly more visible, and shifts to slightly lower voltages, as temperature goes up (see Fig. 3a). This suggests that surface recombination is more important at higher temperatures, while the contribution of other non-radiative recombination mechanisms in the structure increases as temperature moves up.

The effect of device size on surface recombination can be seen in Fig. 3b, where the curves of all devices measured at 100 K are represented. The shoulder associated with surface recombination is more pronounced for the smallest device due to a higher surface-to-volume ratio. As size increases, surface-to-volume ratio decreases and the shoulder becomes smoother, suggesting that other types of recombination start to dominate the LED behaviour. We observed this behaviour at all temperatures measured.

Preliminary measurements on InGaP barrier layers LEDs show much smoother shoulders, i.e. interface recombination is much lower in that kind of devices. However, those devices behave similarly with temperature as the ones studied in this work. This does not allow us to generalise the conclusions from this study yet, but we intend to corroborate the generality of our results in future publications.

3.2 Coupling Quantum Efficiency

An example of the dependence of the CQE on the the applied voltage is shown in Fig. 4a, where the curves corresponding to the smallest device are plotted. The chosen temperatures correspond to room temperature (300 K), the one at which the highest CQE was obtained (250 K) and the lowest temperature measured (100 K). It can be seen that both the maximum CQE and its corresponding voltage change with temperature, with the

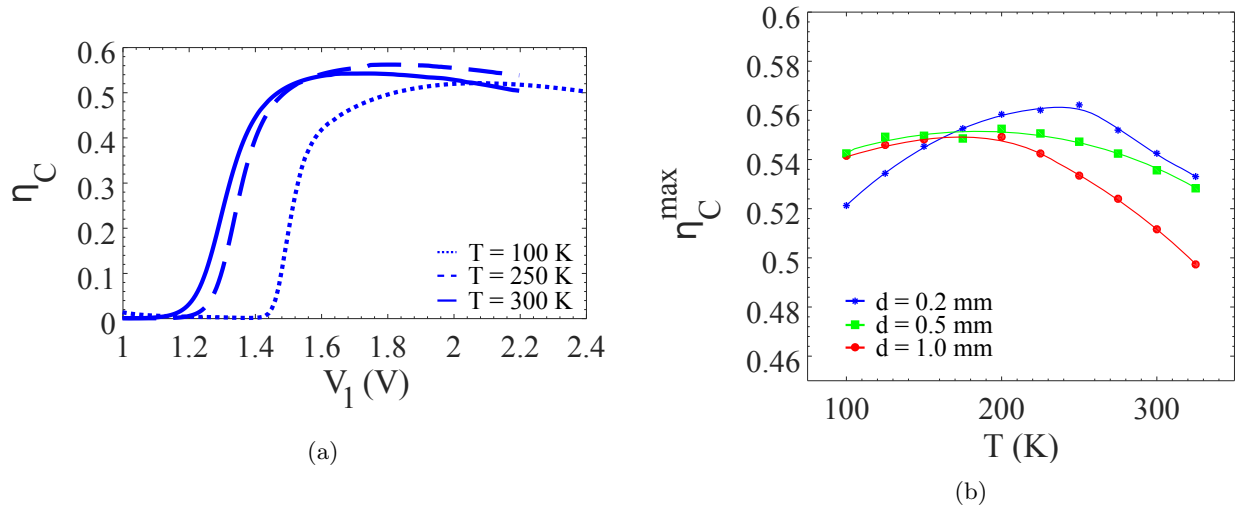

Figure 4: (a) CQE (η_C) dependence on LED bias (V_1) for the smallest device (0.2 mm diamter) at three selected temperatures (see text) and (b) temperature dependence of the CQE peak (η_C^{max}) for the three studied devices.

latter decreasing when temperature increases. We observed a similar behaviour for all of our devices within the measured temperature range.

The temperature dependence of the maximum CQE, η_C^{max} , of the three DDSs is presented in Figure 4b. In all cases, the CQE reaches a peak at temperatures (T_C^{max}) below room temperature. Otherwise, the CQE does not significantly change as temperature goes down to 100 K for the larger devices, while it decreases for the smallest. We also observe the peak of the CQE shifts to higher temperatures as the maximum CQE value increases (T_C^{max} = 250 K for the smallest device with highest CQE and T_C^{max} = 200 K for the rest), although this observation needs further analysis.

The maximum CQE modestly increases for the bigger devices, while it increases more significantly for the smallest device at temperatures ranging from 100 K to T_C^{max}. This could be attributed to a decrease of the surface recombination in the devices mesa edges, as the LED $I-V$ curves show in Fig. 3a. For temperatures above T_C^{max} the CQE goes down as expected, which can be explained by a decrease of the radiative recombination currents, as suggested by early simulations (not shown here), in interplay with an increase of non-radiative recombination, as suggested by figure Fig. 5, showing the A parameter (related to non-radiative recombination) as a function of temperature for the three DDS devices studied.

It is worth noting that these devices are far from being optimised, explaining the low η_C values. However, at present we suspect that a large fraction of the losses originates from the photodetector so that the LED internal quantum efficiency can in fact peak at values close to unity at high biases.[10]

3.3 Power Conversion Efficiency

Figure 6a shows the dependence of the PCE on V_1 for the smallest device (0.2 mm diameter) and the same temperatures (100 K, 250 K and 300 K) as in Fig. 4a. Again, the peak PCE occurs at 250 K. It can also be seen that the voltage corresponding to the maximum PCE becomes lower as the temperature increases.

In figure 6b the maximum PCE is represented for the three devices at all the measurement temperatures. It can be observed that, contrary to the CQE, the higher temperature regime (T_C^{max} – RT) is relatively flat for all devices, albeit the efficiency does show a maximum at around ∼200K.

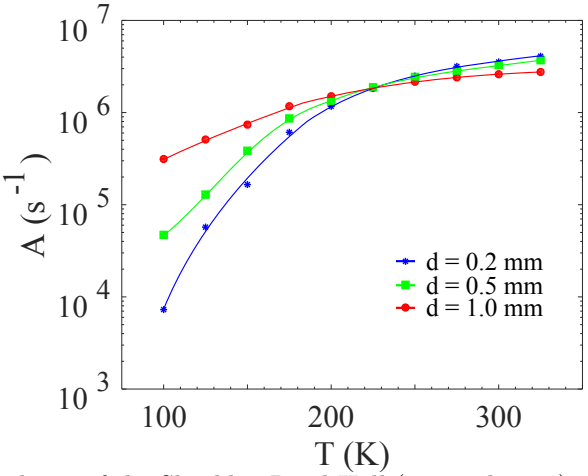

Figure 5: Temperature dependence of the Shockley-Read-Hall (non-radiative) recombination parameter, defined as A in the ABC model, for the three LEDs studied in this work.

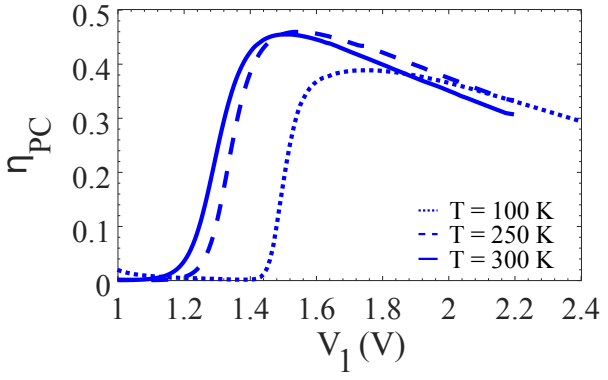

(a)

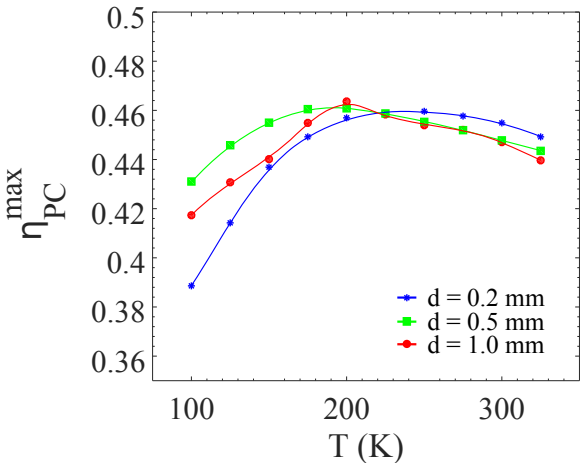

(b)

Figure 6: (a) Example of the behaviour of PCE (η_{PC}) versus LED bias (V_1), for the smallest device at three selected temperatures (see text) and (b) dependence of the PCE peak (η_{PC}^{max}) with temperature.

4. CONCLUSIONS

We found that, for the DDS structures with $Al_{0.3}Ga_{0.7}As$ barrier layers LEDs studied in this work, it is possible to observe higher CQE and PCE values at temperatures below RT. The relative increase seems to be dependent on device size, i.e. larger devices show a more significant increment of both magnitudes. Additionally, the relative CQE enhancement with respect to its value at room temperature is generally higher than that of the PCE.

ACKNOWLEDGMENTS

This project has received funding from the Academy of Finland and the European Research Council (ERC) under the European Unions Horizon 2020 research and innovation programme (grant agreement No 638173). We acknowledge the provision of facilities and technical support by Aalto University at Micronova Nanofabrication Centre.

REFERENCES

[1] Xue, J., Li, Z., and Ram, R. J., "Irreversible thermodynamic bound for the efficiency of light-emitting diodes," *Physical Review Applied* **8** (July 2017).

[2] Santhanam, P., Gray, D. J., and Ram, R. J., "Thermoelectrically pumped light-emitting diodes operating above unity efficiency," *Physical Review Letters* **108**, 097403 (Feb. 2012).

[3] Olsson, A., Tiira, J., Partanen, M., Hakkarainen, T., Koivusalo, E., Tukiainen, A., Guina, M., and Oksanen, J., "Optical energy transfer and loss mechanisms in coupled intracavity light emitters," *IEEE Transactions on Electron Devices* **63**, 3567–3573 (Sept. 2016).

[4] Radevici, I., Tiira, J., Sadi, T., and Oksanen, J., "Influence of photo-generated carriers on current spreading in double diode structures for electroluminescent cooling," *Semiconductor Science and Technology* **1**, 05LT01–1–5 (Mar. 2018). DOI: 10.1088/1361-6641/aab6c3.

[5] Sadi, T., Radevici, I., Kivisaari, P., and Oksanen, J., "Electroluminescent cooling in III-V intracavity diodes: Practical requirements," *IEEE Transactions on Electron Devices* **66** (2019). Accepted, doi: 10.1109/TED.2018.2885267.

[6] Choi, Y.-H., Ryu, G.-H., and Ryu, H.-Y., "Evaluation of the temperature-dependent internal quantum efficiency and the light-extraction efficiency in a GaN-based blue light-emitting diode by using a rate equation model," *Journal of the Korean Physical Society* **69**, 1286–1289 (Oct. 2016).

[7] Park, J. H., Lee, J. W., Kim, D. Y., Cho, J., Schubert, E. F., Kim, J., Lee, J., Kim, Y.-I., Park, Y., and Kim, J. K., "Variation of the external quantum efficiency with temperature and current density in red, blue, and deep ultraviolet light-emitting diodes," *Journal of Applied Physics* **119**, 023101 (Jan. 2016).

[8] Lin, S., Shih, T., Yan, W., Lu, Y., Lin, Y., Chang, R. R., and Chen, Z., "Maximum limits on external quantum efficiencies in bare LEDs," *IEEE Transactions on Electron Devices* **64**, 1597–1601 (Apr. 2017).

[9] Karpov, S., "ABC-model for interpretation of internal quantum efficiency and its droop in III-nitride LEDs: a review," *Optical and Quantum Electronics* **47**, 1293–1303 (June 2015).

[10] Radevici, I., Tiira, J., Sadi, T., Ranta, S., Tukiainen, A., Guina, M., and Oksanen, J., "Thermophotonic cooling in GaAs based light emitters," *Applied Physics Letters* **1**, accepted for publication (2019).